FRICTIONAL DRAG REDUCTION: REVIEW AND NUMERICAL INVESTIGATION OF MICROBUBBLE DRAG REDUCTION IN A CHANNEL FLOW

(DOI No: 10.3940/rina.ijme.2018.a2.460)

S Sindagi, **R Vijayakumar,** Indian Institute of Technology, Madras, India and **B K Saxena**, Tolani Maritime Institute, Pune, India

SUMMARY

The reduction of ship's resistance is one of the most effective way to reduce emissions, operating costs and to improve EEDI. It is reported that, for slow moving vessels, the frictional drag accounts for as much as 80% of the total drag, thus there is a strong demand for the reduction in the frictional drag. The use of air as a lubricant, known as Micro Bubble Drag Reduction, to reduce that frictional drag is an active research topic. The main focus of authors is to present the current scenario of research carried out worldwide along with numerical simulation of air injection in a rectangular channel. Latest developments in this field suggests that, there is a potential reduction of 80% & 30% reduction in frictional drag in case of flat plates and ships respectively. Review suggests that, MBDR depends on Gas or Air Diffusion which depends on, Bubble size distributions and coalescence and surface tension of liquid, which in turn depends on salinity of water, void fraction, location of injection points, depth of water in which bubbles are injected. Authors are of opinion that, Microbubbles affect the performance of Propeller, which in turn decides net savings in power considering power required to inject Microbubbles. Moreover, 3D numerical investigations into frictional drag reduction by microbubbles were carried out in Star CCM+ on a channel for different flow velocities, different void fraction and for different cross sections of flow at the injection point. This study is the first of its kind in which, variation of coefficient of friction both in longitudinal as well as spanwise direction were studied along with actual localised variation of void fraction at these points. From the study, it is concluded that, since it is a channel flow and as the flow is restricted in confined region, effect of air injection is limited to smaller area in spanwise direction as bubbles were not escaping in spanwise direction.

NOMENCLATURE

ACS	Air Cavity Ship
ALDR	Air Layer Drag Reduction
BDR	Bubble Drag Reduction
CFD	Computational Fluid Dynamics
EEDI	Energy Efficiency Design Index
MBDR	Micro Bubble Drag Reduction
PCDR	Partial Cavity Drag Reduction
SWR	Super Water- Repellent
TBL	Turbulent Boundary Layer
R_F	Frictional Resistance of Ship
C_F	Coefficient of Friction
C_{F0}	Coefficient of friction without bubbles
S	Wetted surface area of Ship
U	Speed of ship or Flow speed in pipe
τ_w	Shear Stress
μ	Dynamic Viscosity
$\frac{du}{dy}$	Velocity Gradient
$\rho U'V'$	Reynold's Stress
ν	Kinematic Viscosity
u_0^*	friction velocity of the fully-wetted flow
l_v	Viscous wall unit
$\frac{A_B}{A_{Total}}$.	Ratio of Area of Bubble to the total Area of flow
d_b	Diameter of Bubble
D_P	Diameter of Pipe
Q	Flow of Fluid in Pipe
$C_{f0}(Q_a)$	Corrected C_{f0} at the air flow rate (Q_a)
$U(Q_a)$	Average flow speed at Q_a
α_m	Void Fraction
Q_w	Flow rate of water
Q_a	Flow rate of air
δ	Boundary-layer thickness
δ^*	Displacement thickness,
b	Width of the injector section
t_b	Equivalent air layer thickness
Ba	Width of the plate
H	Height of the channel
C_T	Coefficient of Total Resistance
C_W	Coefficient of Wave making Resistance
F_d	Depth Froude Number
D	Depth of ship
1+K	Form factor
W	Work rate to propel a ship
ΔW	Reduction in Work rate to propel a ship due to injection of bubbles.
W_{pump}	Pumping power for air injection
W_o	Work rate to propel a ship in non-bubble condition
W_{net}	Net work rate to propel a ship in Bubble condition
R_{TO}	Ship's Drag in Non Bubble condition
R_T	Ship's Drag in Bubble condition
H	Water depth at injection point
C_P	Local pressure coefficient at injection point
r_D	Ratio of wave Drag to Viscous Drag
P_{saved}	Net power savings
P_D	Power required to overcome the ship's total drag
η_{Prop}	Propeller efficiency

1. INTRODUCTION

Anybody moving through a fluid experiences resistive force, which is divided into two components: Viscous drag (Frictional drag) and Pressure drag (Form drag or profile drag) (Lewis, n.d). Viscous drag originates from friction between the fluid particles itself and friction between particles of fluid and the surfaces over which it is flowing. The Frictional Drag is a component of Viscous drag, depends on the viscosity of liquid and of course the density. As per 2003 figures (Kim, 2011), worldwide, ocean shipping consumes about 2.1 billion barrels of oil per year. If we can save 30% of the fuel consumption by a flow-control scheme through the frictional drag, it would result in a saving of $38 billion per year (based on $60 per barrel) for shipping industries. It has also been reported by (Watanabe, 1991) that NOx and SOx emissions from ship engines in maritime transport account for 7% and 4% of total NOx and SOx contaminants, respectively, in the entire world. It is reported that, the fluid frictional drag accounts for as much as 60% of the total drag for cargo ship, and about 80% of that for a tanker, thus there is a strong demand for the reduction in the fluid frictional drag.

Numerous technologies (Sindagi, et al, 2016) have been studied and utilized to reduce the frictional drag of a surface. It is concluded that, MBDR has added advantages over other drag reducing technologies, such as environmental friendly, easy operations, low costs and high saving of energy. It is also reported that the MBDR is able to achieve 80% reduction in frictional drag, which can result in a substantial fuel savings for both commercial and naval ships.

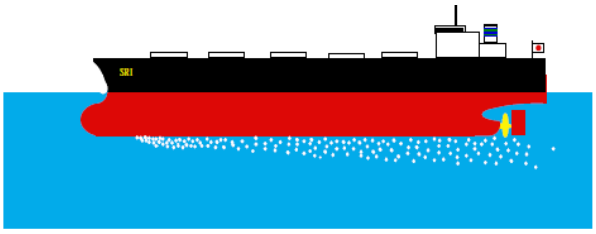

Figure 1 An image of microbubbles applied to a full-scale Ship (Yoshiaki, et al, n.d)

The most significant contribution regarding microbubble drag reduction was presented (McCormick & Bhattacharyya, 1973) by demonstrating hydrogen bubbles generated by electrolysis to reduce frictional drag on a fully submerged body of revolution. Since then, a large number of studies have been carried out on MBDR. As mentioned in the study (Yoshiaki, et al, 2000), Skin friction reduction of full-scale ships has its own difficulties in terms of higher value of Reynolds number and scaling up of skin friction device, which becomes more difficult to apply, along with fouling problem in the sea environment, which makes the application still more difficult. Displacement ships such as tankers especially VLCC & ULCC and Cargo Ships shown in Figure 1 are very large and move very slowly. They are especially suited to MBDR as, their skin friction drag component is about 80% of the total drag and their shape is like a box with wide flat bottom, forcing bubbles injected at the bottom near the bow to stay close to the hull bottom by buoyancy (Yoshiaki, et al, n.d). Thus, the injected bubbles can cover the whole hull bottom efficiently.

The Cement Carrier is also suitable for MBDR (Kodama, et al, 2004) as is generally equipped with blowers and related piping for feeding air to load and unload cement, which can be used to supply air for microbubbles. The energy required for microbubble injection is not small, as large ships have higher values of drafts resulting in escalation of hydrostatic pressure below the hull, which makes injection below hull more energy consuming, thus reducing the efficiency of entire MBDR system. Therefore, it is necessary to reduce the amount of air and/or increase the drag reduction by studying the drag reduction mechanism and minimizing the amount of injected air (Yoshiaki, et al, n.d). MBDR is expected to be suited for slow moving vessels with a target speed range of Froude numbers between 0.05 and 0.15 (MARIN, 2011) and of course to vessels operating in shallow water, where there is reduction in pressure below the hull due to shallow water effect (Sindagi, et al, 2016). Considering the importance and impending obligations, this paper reviews MBDR based on following significant points, which shall become platform for the researchers worldwide.

- Mechanisms inducing the microbubble drag reduction
- Methodology used for microbubble generation and Injection
- Effect of Void Fraction/Flow rate on drag reduction
- Effect of Bubble size distributions and coalescence
- Effect of Surfactant solution and salinity of water on bubble size formation
- Effect of position of Microbubble Injection
- Effect of Depth of water
- Effect of Microbubbles on the performance of Propeller
- Net savings in power considering Power required to inject microbubbles
- Suggestions to improve the drag reduction/ future scope for the researchers

Moreover, work on 3D numerical investigations into frictional drag reduction by microbubbles in Star CCM+ on a channel for different flow velocities, different void fraction and for different cross sections of flow at the injection point are presented in the paper. This study is the first of its kind in which, variation of coefficient of friction both in longitudinal as well as spanwise direction were studied along with actual localised variation of void fraction at these points.

2. MECHANISMS INDUCING THE MICROBUBBLE DRAG REDUCTION

To improve upon the efficiency of MBDR, one must understand the mechanisms by which there is considerable a reduction in the frictional drag. In

alignment with observations of researchers, a close examination of the experimental and numerical results revealed that following mechanisms could be attributed to the reduction in the frictional drag

- Bubble/ Transitional Layer/Air Layer/ Air cavity formation
- Reduction in Density
- Reduction in Reynold's Stress
- Bubble Stratification
- Near wall Phase composition
- Reduction of Turbulence intensity in the Streamwise direction
- Prevention of Formation of spanwise vorticity near the wall

Frictional drag of any body is given by the expression

$$R_F = C_F \frac{1}{2} \rho S U^2$$

From the above expression, it can be concluded that, to reduce the frictional drag, one must reduce the C_F, density of liquid flowing and reduce the wetted surface area. In Bubble Drag Reduction (BDR), as shown in Figure 3, combined effect of density and wetted surface area reduction along with reduction in C_F due to alteration of flow properties and modification of turbulent momentum transport due the presence of bubbles causes considerable reduction in frictional drag (Jinho, et al, 2014). If the amount of injected air increases, air bubbles begin to coalesce into patches that cover the surface continuously, and a transitional air layer is formed, where the patches coexist with air bubbles. Figure 2 shows different mechanisms of air lubrication techniques (Mäkiharju, et al. 2012). If sufficiently high flux of air is injected, transition takes place from a bubbly flow to a Transitional Air Layer (Elbing, et al, 2008). This can be identified, if the microbubbles start coalescing and persistent drag reduction increases to more than 20%. As the air flow is increased further, the fraction of the surface covered by clusters of uneven air layer increases, until finally a continuous layer covers the entire surface, which reduces the wetted surface area. This in turn causes considerable reduction in frictional drag and reaches to almost 80%. In PCDR, a recess is created on the bottom of the hull that captures a volume of gas and creates a cavity of air between the hull and outer flow (Mäkiharju, et al. 2012). Researchers in the former USSR (Butuzov, 1967) (Butuzov, et al, 1999) studied PCDR for decades and developed several ships that utilize this method. These ships are sometimes called ACS or ship with artificial cavity (SAC) (Butuzov, et al, 1999), (Zverkhovskyi, et al, 2015). In the last decade, many research groups have studied PCDR through numerical modelling (Matveev, 2003), small scale experiments (Arndt, et al, 2009) (Gokcay, et al, 2004), and large scale experiments (Lay, et al, 2010), (Mäkiharju, et al. 2012). A recent review by (Ceccio, 2010) discusses relevant topics related to PCDR.

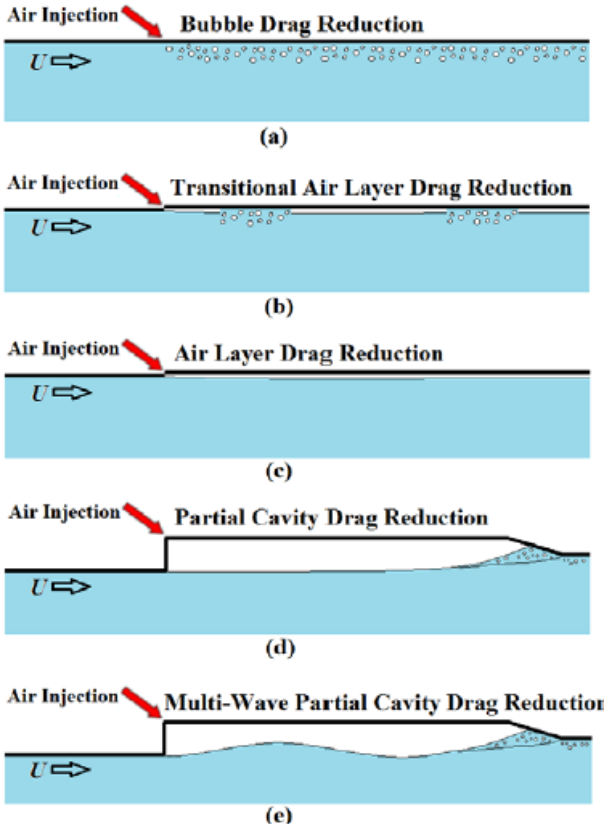

Figure 2 Conceptual sketches illustrating the different air lubrication techniques (Mäkiharju, et al. 2012) & (Jinho, et al, 2014).

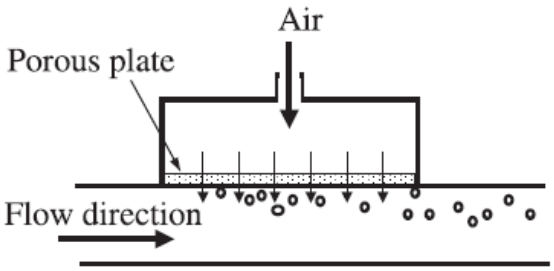

Figure 3 Air injection chamber and bubble generation through a porous plate (Madavan, et al. 1984).

The shear stress developed due to viscosity of liquid can be estimated by using

$$\tau_w = \mu \frac{du}{dy} - \rho U'V'$$

When air bubbles are present, the density of mixture decreases and accordingly shear stress is reduced. The second term in the above equation is Reynolds stress, which reduces as the density (ρ) decreases. It is opined that, (Thomas, et al, 2016), (Madavan, et al, 1984) & (Yoshiaki, et al, n.d) small bubbles or minute particles in liquid increases the effective viscosity of liquid. This originates the increase in first term of above equation. Thus, MBDR is effective only if, reduction in density and in turn reduction in Reynold's Stress is greater than increase in viscosity of liquid. In order for this

mechanism to work, bubbles must be very small with diameter ranging from 0.5mm to 1mm. However, there is a possibility that much smaller bubbles can also contribute to reduction in frictional drag. The study by MARIN's research projects (Foeth, n.d), PELS (Project Energy-saving air-Lubricated Ships) and SMOOTH (Sustainable Methods for Optimal design and Operation of ships with air lubricated Hulls) pointed out that, when the bubbles are within 300 viscous wall units (l_v) —defined as below, then reduction effect can be seen.

$$l_v = \frac{v}{u_0^*}$$

Where,

$$u_0^* = \sqrt{\frac{\tau_w}{\rho}}$$

As per the study carried out by (Mohanarangam, et al, 2009), it pointed out that, an additional momentum source caused due to the injection of gas redistributes the flow structure within the boundary layer, which increases the normal water velocities and in turn noticeable reduction in the mean streamwise velocities. Secondly, the presence of the micro-bubbles causes appreciable turbulence modification or the turbulence suppression effect results in considerable reduction in the frictional drag. The formation of a low-void-fraction layer, e.g. bubble stratification (Sanders, et al, 2006), has been observed when buoyancy acts to move microbubbles away from the solid surface when plate of observation is placed below. Conversely, buoyancy can lead to the formation of air layer when it forces microbubbles onto the plate surface. At higher speeds, fluctuating lift and drag forces on the individual microbubbles can overcome buoyancy, and the process of turbulent diffusion and mixing dominates and in turn loss in the drag reduction. Sanders, et al (2006) and Moriguchi & Kato, (2002) observed that, near wall Phase composition plays an important role in the MBDR. There is a strong relationship between the concentration of bubbles near the wall and the drag reduction which depends on the observed area ratio, $\frac{A_B}{A_{Total}}$, void fraction with small bubbles in close proximity to the wall. Figure 4, depicts the distribution of the local void ratio and the mean void ratios (Moriguchi & Kato, 2002). It seems that microbubbles gather in the centre of the channel when the mean void ratio is large. It is concluded (Kitigawa, et al, 2005) that, when the microbubbles are injected, the liquid turbulence intensity in the streamwise direction is decreased slightly in a few regions while that in the wall-normal direction decreases slightly in the whole of the region. The observation of the vortical structure (Kanai & Miyata, 2001) indicates that, injection of microbubbles prevents formation of sheet-like structure of the spanwise vorticity near the wall. The bursting phenomenon of turbulence is depressed as the streamwise vorticity (streamwise vorticity is considered to be created from the spanwise vorticity) is detached from the wall which causes weakening of streamwise vorticity. Accordingly, the low-speed streaks below the detachment position of the spanwise vorticity disappeared, in turn, the turbulent energy is reduced causing reduction in the frictional drag.

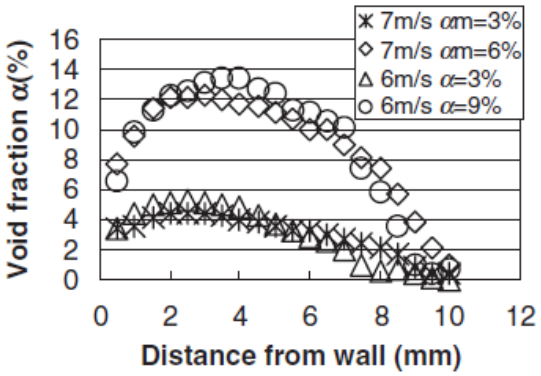

Figure 4 Distribution of Bubbles for different flow speeds (Moriguchi & Kato, 2002)

3. METHODOLOGY USED FOR MICROBUBBLE GENERATION AND INJECTION:

Since generating microbubbles needs energy, it is necessary to optimize the size of the bubbles and their distribution in the boundary layer in order to achieve a net gain in frictional drag reduction. It is anticipated that, bubbles larger than a certain diameter have no effect on frictional drag reduction (Kato, et al, 1998). Literature survey suggests that, following different methods were proposed and tested to generate smaller size of bubbles.

- Porous material (Figure 3)
- 2D convex shape with an ejection hole (Figure 5(a)
- 2D convergent-divergent nozzle with an ejection hole at the throat (Figure 5(b)
- Transverse wire (Figure 5(c))
- Change of Channel height at the point of Bubble Injection (Figure 6)
- Using an air injection plate with an array of air-injecting holes
- Foaming of dissolved water
- Use of Venturi tube

The most commonly practised method to generate microbubbles is by making use of Porous material, where in, air is injected into the flow through the porous medium. Although intuition suggests that, the pore size would be an important parameter, however, literature survey indicates that, the bubble size and in turn the reduction in the frictional drag is not determined primarily by the size of the pores used for injection, but by the characteristics of the flow. Madavan, et al, (1987) used two widely different pore sizes, 0.5mm and 100mm and found that, pore size does not have any substantial effect on the skin-friction results for the conditions tested. These results are of practical importance since

with the larger-pore-size material, less energy is needed to inject microbubbles. (Yoshiaki, et al., 2000) pointed out that with porous material, generated bubbles do not uniformly distributed on the porous plate. In order to solve above problem, a new plate called plate with array of-holes was used (Yoshiaki, et al., 2000). From the experiment it is confirmed that, skin friction reduction by the array-of-holes plate is comparable to that by the porous plate. (Kato, et al, 1998) used three devices shown in Figure 5(a), Figure 5(b) Figure 5(c) for generating smaller size of bubbles. The bubbles downstream of the 2D convergent- divergent (Figure 5(b)) diffuse rather rapidly as the flow separates at the divergent part of the nozzle, which is completely undesirable. Among the three methods used, the 2D convex section shown in Figure 6(a) seems the best for drag reduction by microbubbles as the diameter of the bubbles became about one-third the size of the reference ejection on a flat plate.

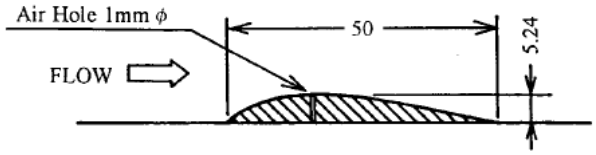

Figure 5(a) 2D convex section with air hole

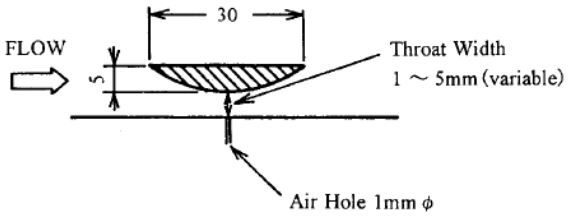

Figure 5(b) 2D convergent- divergent nozzle

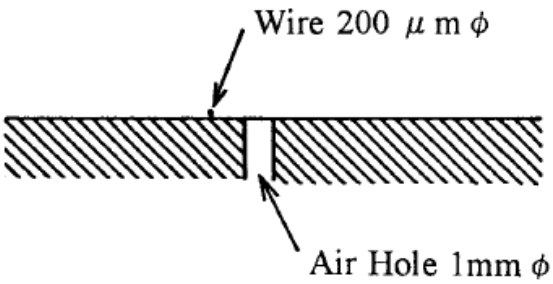

Figure 5(c) Transverse wire

Figure 5 Methods used for the generation of different sized Bubbles (Kato, et al, 1998)

Another way by which size of microbubbles was changed by using three different channels shown in Figure 6 (Moriguchi & Kato, 2002). To change size of microbubbles, flow velocity was altered by choosing different channel heights. Channel 1 has an air injection channel height of 10 mm, Channel 2 has an air injection channel height of 5mm and Channel 3 has an air injection channel height of 20mm. From the experiment it was found that, channel 2, where the channel height was small, generates smaller bubbles than other two channels. As shown in the Figure 7 and as per the empirical relation below, the mean microbubble diameter reduces as the main flow velocity at the injection point is increased.

$$\frac{d_b}{D_P} = 2.4\sqrt{\frac{Q}{UD^2}}$$

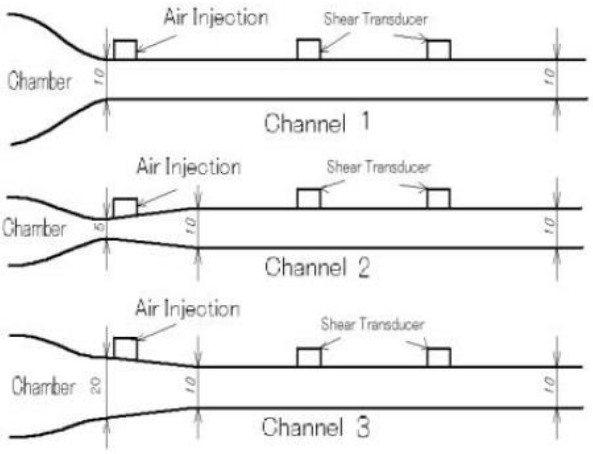

Figure 6: Change of channel height at the air injection point (Moriguchi & Kato, 2002)

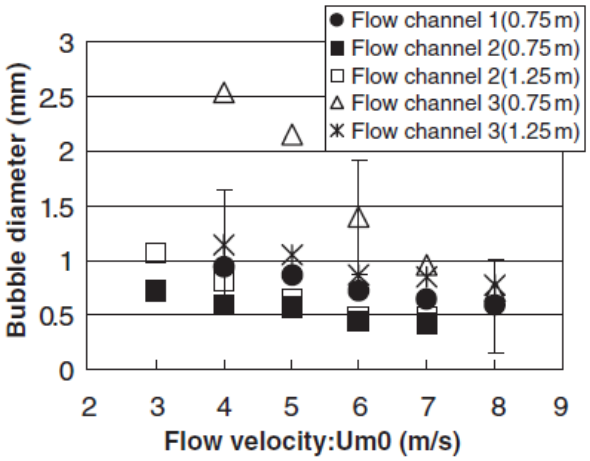

Figure 7 Effect of main flow velocity on mean microbubble Diameter (Moriguchi & Kato, 2002)

Technique with a convergent-divergent nozzle shown in Figure 8 known as venturi tube (Kitigawa, et al, 2005) & (Kawashima, et al, n.d) was introduced. As shown in Figure 8, the liquid velocity at the throat increases and the pressure is decreased, which in turn reduces the size of microbubbles.

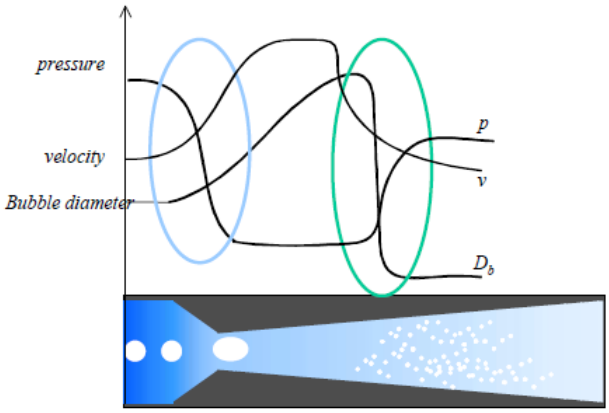

Figure 8 Schematic of venturi tube (Kitigawa, et al, n.d)

Another type of injector is used by (Shen, et al, 2006) to generate smaller bubbles is shown in Figure 9, wherein compressed nitrogen and lipid bubbles are forced through the injector by a manifold with seven evenly distributed ports in the cross-stream direction. As shown, the injector is also placed at angle of 15^0 to flow, which simply helps in evenly distribution of bubbles below the plate.

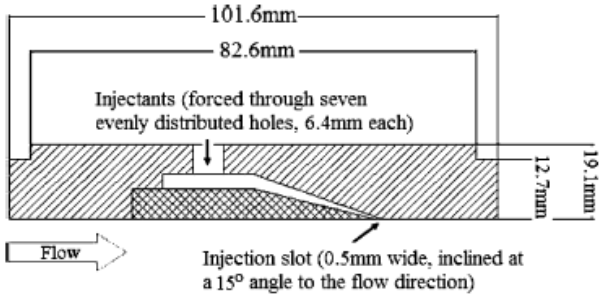

Figure 9 Cross-section schematic of the injector. (Shen, et al, 2006).

4. EFFECT OF VOID FRACTION ON DRAG REDUCTION

It has been proved experimentally and numerically that, MBDR depends on the air flow fraction or commonly known as Void fraction. In fact, research mentions MBDR in terms of void fraction. The air flow fraction or Void fraction is defined as the ratio of volumetric flowrate of air divided by the total flow rate in the boundary layer

$$\alpha_m = \frac{Q_a}{Q_a + Q_w}$$

Where, $Q_w = U(\delta - \delta^*)b$

Measurements of the cross-stream variation of the bubble volumetric concentration at various locations along the surface (Madavan, et al, 1984) & (Madavan, et al, 1983) concludes that, the bubble concentration starts from zero near the wall, increases rapidly to a peak value of 0.6 and at some locations increases to 0.8, and then falls off gradually again to zero in the free stream. For the plate above the boundary layer, substantial skin-friction reductions persist for some 35δ for low air flow rates and up to 60δ -70δ for high air flows. For the plate below the boundary layer, the reductions persist for somewhat shorter distance of 50δ. The persistence of the skin-friction reduction beyond the location of microbubble injection is a function of the gravitational orientation of the plate and the freestream velocity (Madavan, et al, 1985). The local void fraction was measured in an experiment (Kawashima, et al, n.d) & (Takahashi, et al, 2001). Typical observations are presented in Figure 10, which are in line to observations made by Madavan, et al, (1985).

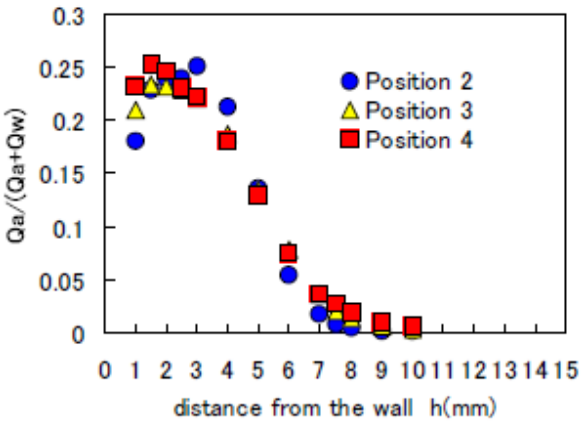

Figure 10 Local void ratio (Array-of-holes plates) (Takahashi, et al, 2001)

The local skin-friction measurements with microbubbles is generally presented in terms of the skin-friction coefficient, C_F, normalized to the corresponding skin friction coefficient without microbubbles, C_{F0} as a function of the void fraction as presented by (Kitigawa, et al, n.d), (Madavan, et al, 1985), & (Wu, et al, 2008). Typical variation obtained from the experiments is presented in Figure 11.

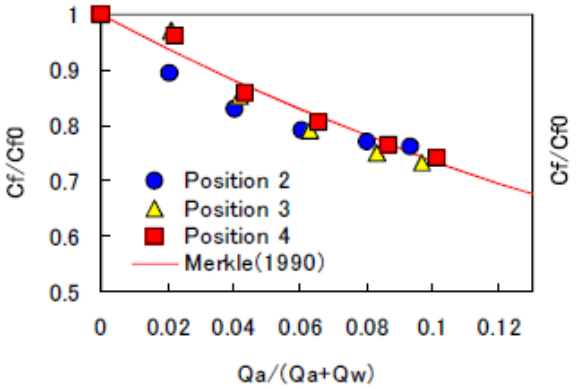

Figure 11 Skin friction reduction by (Moriguchi & Kato, 2002)

5. EFFECT OF FLOW RATE (AIR INJECTION) ON DRAG REDUCTION

As mentioned earlier, it is proved that, MBDR depends on the Void fraction. However, as per the formula of void fraction, it also depends on the injection flow rate of

air. Thus, it is common interest of all researchers to understand the effect of changing flow rate on the frictional drag reduction. Figure 12 describes the relationship between the injection airflow rate and the drag reduction effect at different flow speeds (Wu, et al, 2008). As shown, as the airflow rate increases, the reduction effect increases. However, drag reduction effect start dropping when the airflow rate exceeds the critical value. Possible reason could be, excessive microbubble injection destroys the favourable turbulent boundary layer and in doing so decreases the drag reduction effect.

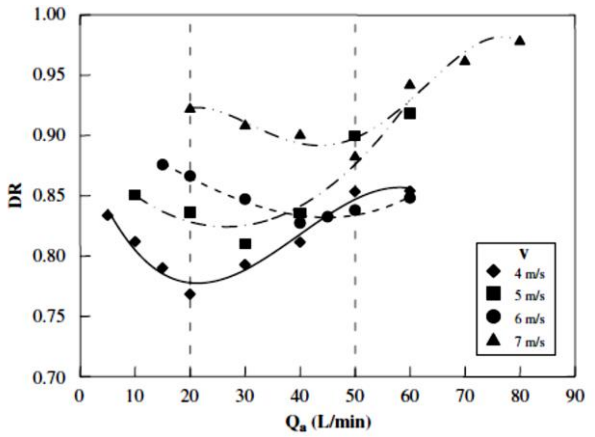

Figure 12 Effect of air injection on drag ratio (Wu, et al, 2008).

It is a common practise to express air injection flow rate into the air layer thickness using the expression

$$t_b = \frac{Q_a}{B_a U}$$

World's first trial on newly built carrier was conducted by (Mizokami, et al, 2010) in a seakeeping tank at MHI's Nagasaki Research & Development Centre. The trial test was carried out by varying air blow-off rate with the equivalent air thickness as 3mm, 5mm and 7mm. Table 1 shows the effect of air layer thickness on the drag reduction effect, which shows that, drag reduction effect increases with increasing air layer thickness and in turn on injection flow rate.

Table 1 Effect of Flow rate on Air Layer thickness and intern effect on Drag Reduction (Mizokami, et al, 2010)

Air Layer Thickness	Net energy-saving effect
7mm	12%
5mm	10%
3mm	8%

6. EFFECT OF BUBBLE SIZE DISTRIBUTIONS, COALESCENCE, STRATIFICATION AND DEFORMATION EFFECT ON DRAG REDUCTION

The intuition says that, the bubble size is one of the major factor which influences the reduction in the frictional drag. Actually, the bubble size depends on how the injected air or gas stream interacts with the local flow structure. From MBDR experiments carried out by (Shen, et al, 2006) (Winkel, et al, 2004), it is found that bubbles were generated by the injection of air or gas through either a slot injector or a porous plate. It is mentioned that; the importance of bubble size can be readily established by considering the ratio

$$d^+ = \frac{d_b}{l_v}$$

In TBL flows, the buffer region extends between $5y^+$ to $30y^+$ (where, $y^+ = \frac{y}{l_v}$ and y is the wall normal coordinate or normal distance from the wall or plate). If the bubbles injected in the buffer layer are smaller than or comparable to a viscous wall unit, then the bubbles will reduce the water density as they are smaller than the size of an overturning eddy. On the other hand, if the bubbles are much larger than $30l_v$, it may not be possible for them to alter the fluid momentum exchange in the buffer layer unless they are present in sufficient number to substantially increase the buffer layer thickness. In the nitrogen injection test (Shen, et al, 2006), the bubble size was varied from 476µm in fresh water, to 322µm in a 20ppm Triton X-100 solution, to 254µm in a 35ppt saltwater solution. From the experimental results, it is concluded that, MBDR is strongly related to the injected air or gas volumetric flow rate and the static pressure in the boundary layer and does not depend on the bubble size. Figure 13 shows the effect of the mean microbubble diameter on the frictional resistance reduction (Moriguchi & Kato, 2002).

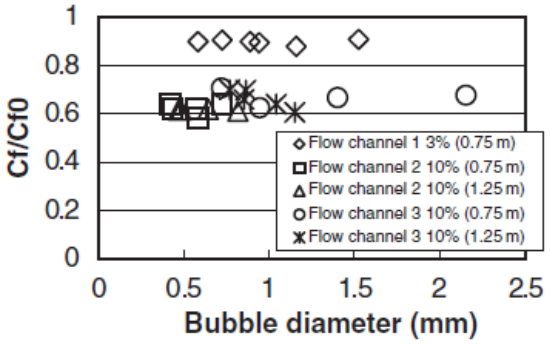

Figure 13 Effect of mean microbubble diameter on frictional resistance reduction (Moriguchi & Kato, 2002)

In another experiment by (Sanders, et al, 2006), bubble sizes and the extent of bubble coalescence was varied with downstream distance and flow speed. It is observed that, for slow speeds, the injected bubbles coalesced into an

intermittent or continuous air film and at higher speeds, discrete bubbles were observed all along the plate. It is also observed that, for both lower and higher flow speeds, the mean bubble diameter increases by an average of about 30%, while the number density decreases by 50% to 80%. Contradictory observations were made by (Thomas, et al, 2016), where it is mentioned that, bubbles of a few millimetres in diameter increased the frictional resistance. It has happened possibly because of the turbulence generated by the wake of bubble. The research work also pointed that, the bubble size is a critical factor in deciding the drag reduction and it will be achieved when the bubble diameter is less than about 1 mm; and the drag reduction rate is generally higher when the bubble diameter is smaller. SR 239 Research Committee performed a full-scale experiment using the Seiun-Maru (Kato & Kodama, 2003). From the experiment, it is concluded that, the ejected air bubbles did not stay in the inner region of the boundary layer well and did not spread thinly over the hull but flowed like chimney smoke and they were slightly away from the hull surface. Also, it is interesting to note that, the air ejection rate was not maximum when the best result was obtained. By considering all these results, it is concluded that, the location of bubbles in the boundary layer is extremely important for the skin friction reduction. In other words, microbubbles are very effective in reducing skin friction, if they can be concentrated in the inner region of the boundary layer, close the wall.

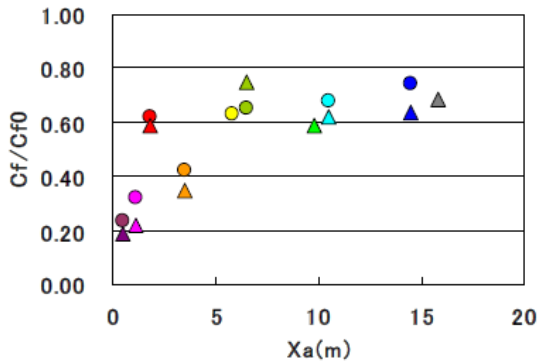

Figure 14(a) Streamwise direction

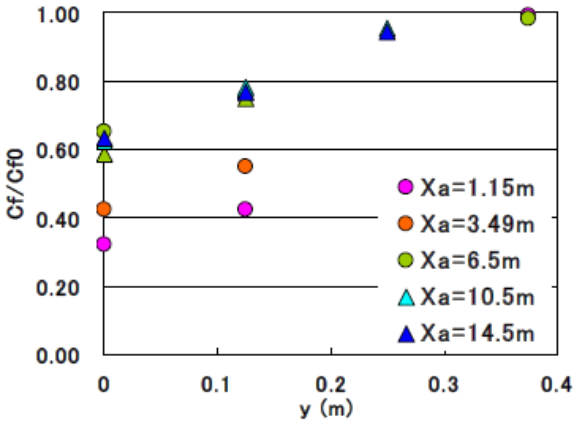

Figure 14(b) Spanwise direction

Figure 14 Distribution of skin friction (Kodama, et al, 2004)

As per the experiment conducted by (Kodama, et al, 2004) to determine the drag reduction effect in streamwise and spanwise direction, it is concluded that, as shown in Figure 14(a), the reduction effect quickly reduces at immediate downstream of injection and shows gradual reduction further downstream. As shown in Figure 14(b), there is no constant reduction region and that the reduction reduces linearly towards the side end spanwise, which suggests that injected bubbles steadily diffuse toward side ends and are lost steadily across them. It is also concluded that, the orientation of the wall also affects drag reduction. The wall-on-top condition gives the largest reduction. This can be easily explained by the fact that the bubble buoyancy favourably effects on the reduction. SWR surface paint was used by (Fukuda, et al, 2000), which is capable of forming a thin air film over an underwater surface and can stop the surface from becoming wet. Due to the surface tension of the water, the air film formed over the surface has the property of being able to take in air supplied. When air is supplied from the bow section to a ship's hull coated with SWR paint, it becomes attached to the SWR surface and forms an air film on it. Figure 15 shows a schematic view of a 7.2-m-long wooden scale model of a 280000-ton VLCC equipped with the SWR. The frictional drag on the SWR surface of the tanker bottom is reduced by about 40% at Froude number 0.20.

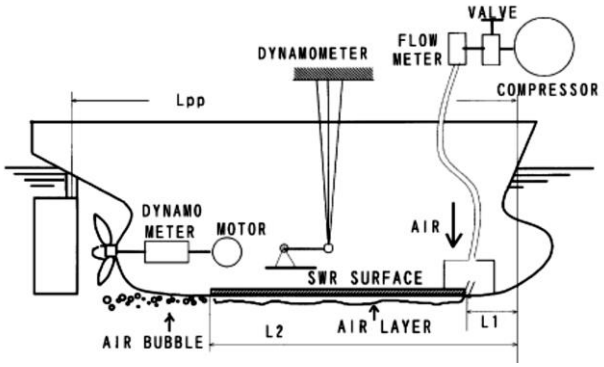

Figure 15 Schematic view of a model ship equipped with the SWR & A technique (Fukuda, et al, 2000)

7. EFFECT OF SURFACTANT SOLUTION AND SALINITY OF WATER ON BUBBLE SIZE FORMATION

It is also important to note that, for the application related to ships, friction drag reduction is sought mostly for the open sea with salt and other surfactants, majority of experiments on MBDR were conducted under laboratory conditions with fresh water. In a particular study carried out by (Shen, et al, 2006), under different aqueous conditions, it found that, the average bubble size was reduced by a factor of 2 in the surfactant solution and by a factor of 4 in saltwater. Table 2 gives the information about the bubbles sizes produced in different aqueous conditions, which clearly shows reduction in the diameter of bubbles produced with increase in the salinity of water.

Table 2 Basic properties of the bubble size for each drag reduction experiment (Shen, et al, 2006).

Aqueous conditions	**Mean (μm)**	**d^+**
Water nitrogen injection	476	200
20 ppm Triton X-100 nitrogen injection	322	134
35 ppt Saltwater nitrogen injection	254	106
Lipid bubble injection	44	18

Experiments were performed by (Winkel, et al, 2004) in freshwater (tap water), at four different concentrations of saltwater (Instant Ocean, Aquarium Systems), and at three different concentrations of a soluble surfactant (Triton-X-100, Union Carbide). Saltwater concentrations of 9, 19, 33 and 38 parts per thousand (ppt) were investigated.

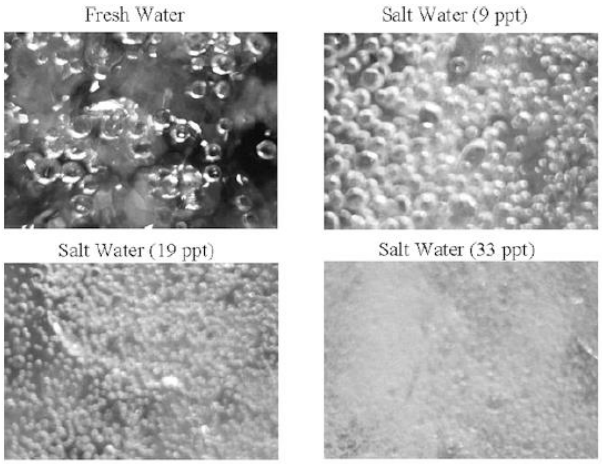

Figure 16 Sample photographs for all the bubble injection conditions tested (Winkel, et al, 2004)

Figure 16 Shows the sample photographs of bubble population, taken near the wall. From the photographs, it can be concluded that, as the solute concentration increases, the bubbles become smaller in size, and are also more evenly distributed over the viewing area. In another experiment conducted by (Takahashi, et al, 2001), CTAC was added to water with concentration up to 40ppm for the speed range up to 10m/sec. Figure 17 shows skin friction reduction as a function of average void ratio at three different CTAC concentration, at one speed of V=5m/sec. It is observed that, the effect of CTAC on skin friction reduction is very small at this flow speed.

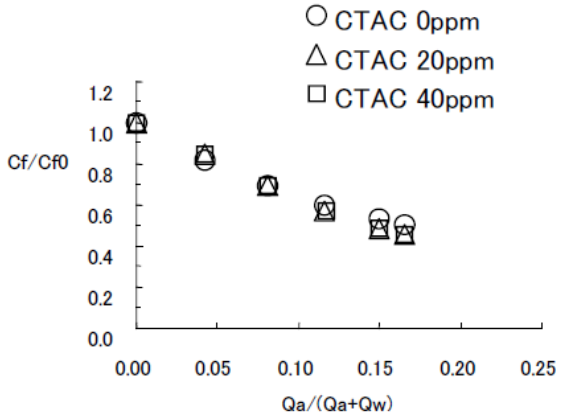

Figure 17 Relation between average void ratio and skin friction ratio ta v=5m/s sec (Takahashi, et al, 2001).

Winkel, et al, (2004) concluded that, one of the physical mechanisms for the reduction in bubble size is probably due to the ionic repulsion between bubbles in saltwater that prevents bubble coalescence near the injector reducing the mean bubble diameter with reduction in surface tension.

8. EFFECT OF POSITION OF MICROBUBBLE INJECTION POINT ON DRAG REDUCTION

Micro bubble injection location is one of the important parameters that need to be considered in reviewing the effectiveness of skin friction reduction by micro bubbles. Resistance tests of the 66K Supramax bulk carrier were performed at design draft to investigate MBDR effect (Yoshiaki, et al, 2000). Six air injection units that operate independently were analysed as shown in Figure 18. Figure 19 represents total percentage reduction in the ship's resistance (ΔR_{TM}) as compared to when air was not injected. It is understood that, a transitional air layer was well developed over the wide area of the bottom as shown in the captured image of Figure 20. However, it was observed that air leakage around the 12th station has caused an additional increase in the resistance by disturbing the flow around the hull.

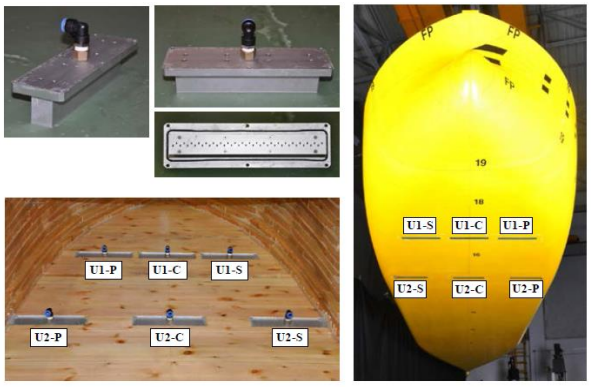

Figure 18 Arrangement of air injection units (Yoshiaki, et al, 2000)

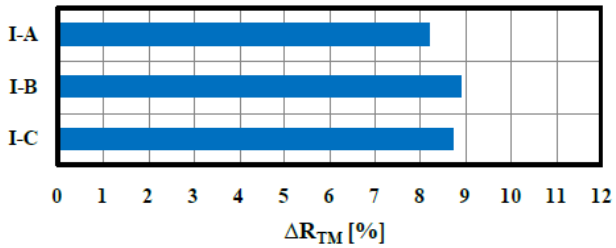

Figure 19 Reduction in the resistance and effective power at VS = 14.5knots (Yoshiaki, et al, 2000).

Figure 20 Captured air layer at VS = 14.5knots (Yoshiaki, et al, 2000)

Secondly, air was injected from the only centre injection units at the same towing speed as the previous case. These Results shown in Figure 21 conclude that, more resistance reduction was attained when air was injected from the centre units only, compared to the case of air injection from all units including the side. In other words, the side injection units did not make any contribution to the reduction in the resistance.

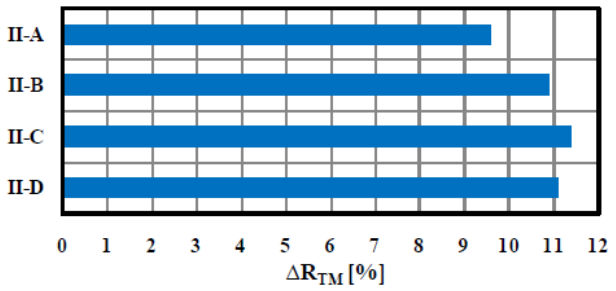

Figure 21 Reduction in the resistance and effective power at VS = 14.5knots (Yoshiaki, et al, 2000)

A series of model tests were conducted on a navy fast patrol boat (FPB) for a Froude number of up to 0.65 by (Sunaryo & Jamaluddin, 2012) and (Thomas, et al, 2016). The influence of the location of micro bubble injection and bubble velocity was investigated in both experiments. Figure 22 shows the lines plan for test model and the positions of bubble injectors placed behind the mid-ship. Positions varied from position 1, position 2, and position 3. These positions were investigated and compared regarding the influence of micro-bubble injection. Position 1 was 5 cm in front of the midship, position 2 was exactly at midship, and position 3 was 5 cm behind the midship. From the experimental results as shown in Figure 23, it was found that, the ship model with bubble injection at position 3, has a smallest value of C_T and found that the skin friction reduction is highest when the position of bubbles was located at the rear. It is clear that drag reduction for position 3 is greater than position 1 and position 2.

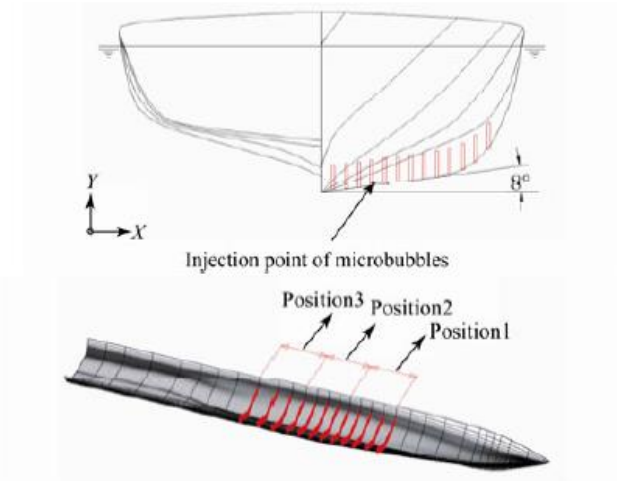

Figure 22 Lines plan and positioning bubble injector (Sunaryo & Jamaluddin, 2012)

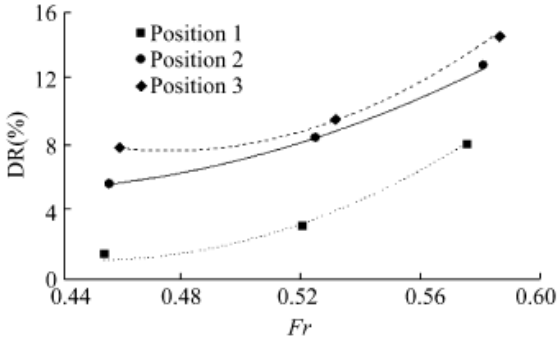

Figure 23 Relationship between drag reduction and Froude Number (Sunaryo & Jamaluddin, 2012)

9. EFFECT OF DEPTH OF WATER ON REDUCTION IN FRICTIONAL DRAG

In the nitrogen injection test by (Shen, et al, 2006), the bubble size was varied from 476 μm in fresh water, to 322 μm in a 20 ppm Triton X-100 solution, to 254 μm in a 35 ppt saltwater solution. From the experimental results placed at Figure 24, it can be concluded that, the most important parameter in determining MBDR effect is the effective gas phase volumetric flow rate, which is influenced both by the injection rate and the static pressure under the test conditions i.e. the pressure of water flow. Increasing the static pressure causes the volumetric flow rate of the injected gas phase to decrease proportionally. These results show that when using void fraction to compare MBDR results, the gas volumetric inflow rate must be corrected for the static pressure in the test section. Moreover, the efficiency of the same would decrease significantly with increasing depth if all other parameters are held constant.

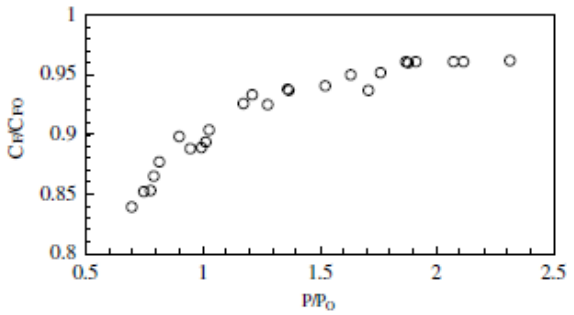

Figure 24 Effects of static pressure on friction drag reduction. Tap water with nitrogen injection, plate-on-top (Shen, et al, 2006)

As per the study carried out by (Yoshiaki, et al, n.d), to increase the MBDR effect, it is recommended to increase Froude number based on depth of water, which is given by $F_d = \frac{U}{\sqrt{gD}}$. It suggests that, either increase the flow speed and/or operate the vessel in shallow water, as it may require less work for the injection of air. (Mäkiharju, et al, 2012) stated that, the cost of pumping the air goes up with the square of the draft, since an increase in draft increases both the back pressure against which the compressor or blower must work, and the required mass flux of air and the gas volume must be compressed when injected into the higher-pressure flow beneath the hull.

10. EFFECT MICROBUBBLES ON THE PERFORMANCE OF PROPELLER

It is anticipated that, injection of bubbles below the hull will interfere with the operation of propeller and may reduce its efficiency. It is also expected that, it might increase the cavitation effect. Considering above, researchers worldwide are keen in finding out the effect. To investigate effects of air layers on the propulsion performance, self-propulsion tests of the 66K Supramax bulk carrier were performed by (Jinho, et al, 2014). From the experimental result, it is detected that, the axial velocity increased significantly and the nominal wake fraction, has reduced. Moreover, it was observed that, downward flow in the upper area of the propeller shaft has reduced. It is thought that, increase in the momentum of the flow along the hull bottom by the reduction in frictional drag accelerated flow into the propeller plane and this might have led to the reduction in the propeller thrust and torque. Experimental results also confirm that, relative rotative efficiency is reduced by less than 1%, hull efficiency decreased by about 5~6%, but open water efficiency increased by about 5% as the propeller loading was reduced. Consequently, the quasi-propulsive efficiency was reduced by about 0.6~0.9% and finally, the delivered power was reduced by 7~9.5%. Similar observation was made (Kato & Kodama, 2003), where the efficiency of the propeller was reduced by 3%-6% by the air ejection. It is opined that, the reduction in the thrust generated by the propeller was due to the reduction in the density of flow by injection of air. From the study by the Mitsubishi Air Lubrication System (MALS) (Kawabuchi, et al, 2011), significant observations were made. It was found that, the amount of air bubbles flowing into the propeller disk area decreased as the air bubble diameter increased. This may have been due to the buoyancy force, which increased with the air bubble diameter. However, the peak position of the void fraction did not vary substantially with the air bubble diameter. Judging from the average void fraction distribution on the propeller disk, the propeller efficiency of this ship remained nearly unchanged by the bubbles. Furthermore, it is predicted that, the intrusion of bubbles on the area of propeller disks, which could deteriorate the performance, and confirmed that the deterioration in propeller disk performance was negligible. Experiments have been performed by (MARIN, 2011) on ships with and without air-bubble injected at model and full scale. The results of model scale experiments showed a small increase in resistance and a small increase in propulsion efficiency, both around 1-2%. A trial with the ship with air injection at full scale showed 2.6% reduction in required propulsive power with air.

11. NET SAVINGS IN POWER CONSIDERING POWER REQUIRED TO INJECT MICROBUBBLES AND EFFECT ON PROPELLER PERFORMANCE

In order to evaluate the applicability of MBDR method to ships, it is essential to discuss its net drag reduction effect by taking into account the energy required to inject air or gas bubbles into water. Simplest format for estimating the net savings in the work, was given by (Kodama, et al, 2004).

$$Savings_{net} = \frac{W - W_{Pump}}{W} = \frac{(\Delta W)}{W}$$

Using the equations derived above, net savings in power for the cement carrier was estimated and it was found that, the drag of the ship in the fully loaded condition decreased by 7.38%. The pumping power needed for injecting air was found to be 1.94% and hence the net power-saving found to be 5.44%. Yoshiaki, et al, (n.d) proposed modified and upgraded methodology to predict net power savings, wherein, it was proposed to calculate net work (r_w) ratio as follows

$$r_w = \frac{W_{net}}{W_o} = \frac{R_T U + W_{Pump}}{R_{TO} U} = \frac{R_T}{R_{TO}} + \frac{W_{Pump}}{R_{TO} U}$$

Where,

r_w=1.0 when net drag reduction is zero
r_w<1.0 when there is drag reduction effect

W_{Pump} is expressed by taking into account energy loss due to head pressure at injection point and the local pressure there. Ship's Drag in non-bubble condition can be expressed in conventional non-dimensional form

$$R_T = [(1+K)C_{Fo} + C_W] * \frac{1}{2}\rho S U^2$$

Thus, by putting relevant expressions, we get

$$r_w = \frac{R_T}{R_{TO}} + \frac{W_{Pump}}{R_{TO}U}$$

$$r_W = \frac{r_D + \frac{\overline{C_{FO}}}{C_{FO}}}{1+r_D} + \frac{Q_a}{SU_\infty}\frac{C_P + \frac{2}{F_d^2}}{(1+K)C_{FO}(1+r_D)}$$

Where,

$$r_D = \frac{C_W}{(1+K)C_{FO}}$$

Based on the experiments carried out by (Jinho, et al, 014), as shown in Figure 25, the net power savings, was estimated to be 5~6% in the speed range of 13.0~16.0knots, which is in line to observations made earlier.

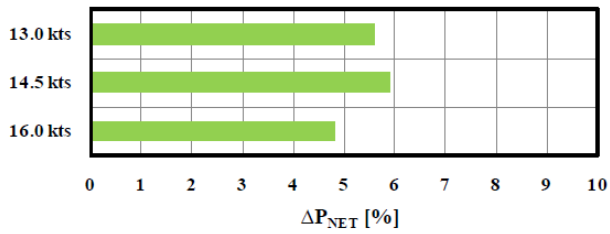

Figure 25 Net power savings at mean tAL = 8.2mm (Jinho, et al, 2014)

Mäkiharju, et al, (2012) presented an energy cost-benefit analysis for ALDR and PCDR for a ship with a large flat bottom. It was assumed that the ship's form drag is not appreciably changed by the air injector and the air layer persists along the entire length of the hull. Only the fraction of the ship's energy consumption for propulsion is considered in order to develop the possible net power savings, $\%P_{saved}$, compared to the power consumption required to pump the lubricating air:

$$\frac{\%P_{Saved}}{100} \cong \frac{P_{saved}}{P_D/\eta_{Prop}}$$

The net work ratio is estimated for a large tanker with 300m length and the speed of 14kts (Yoshiaki, et al, n.d). From the experimental and theoretical analysis, the net work ratio was calculated as 1.078, which is slightly greater than 1, which means that net drag reduction is not obtained. On the other hand, in the ballast condition (empty condition), the draft reduces and hence the r_W reduces to 0.979, approximately 2% net reduction was obtained. This means that, a tanker that runs between Japan and the Middle East can get net drag reduction one way. If the amount of air can be economized to half, the net work ratio becomes 0.952 even at full load condition. In general, in order for an energy-saving effect not to be embedded into measurement errors, it has to be 5% at least. This rough estimation suggests that, in order to put microbubbles into practical use, it is necessary to improve drag reduction efficiency at least twice as much and/or to combine the technique with other efforts such as developing a new hull form suited for microbubbles like one with very shallow draft and very wide flat bottom.

12. NUMERICAL INVESTIGATION ON CHANNEL FLOW

The experimental study was conducted by (Moriguchi & Kato, 2002) using recirculating water channel as shown in Figure 26. The test section, which is 10 mm high, 100 mm wide, and 2000 mm long generates a fully developed turbulent flow. Compressed air is injected into the channel for different flow rates and its effect is measured using shear stress transducers placed at 750mm and 1250mm from the injection point. Similar setup is used here to enhance the study using CFD technique. 3D numerical investigations into frictional drag reduction by microbubbles are carried out in Star CCM+ in a channel for different flow velocities, different void fraction and for different cross sections of flow at the injection point. The experimental investigation was carried at only two longitudinal locations and no observation was made at spanwise locations, which is easily possible in CFD technique. In the numerical setup, microbubbles were injected through series of holes of 1mm in diameter in the test section at the upstream upper surface, generating air–liquid flow. Coefficient of friction and void fraction values were measured at 12 longitudinal positions and at each longitudinal position, 11 in number transverse and depth wise positions were observed. In all, for one simulation, data at more than 1000 positions were collected. Simulations were performed at flow velocities ranging 4–7 m/s in the interval of 1 m/s, and at different air flow rate (12 values of Void fraction). More than 60 simulations were carried out to study the effect of these flow parameters on coefficient of friction. Effect on C_F was also studied by changing the depth of channel at the injection point, which changes flow parameters.

12.1 NUMERICAL SETUP & VALIDATION WITH EXPERIMENTAL RESULTS

The numerical and mesh setup used for this exhaustive study is shown in Figure 26 & Figure 27. Grid independency study was also carried out to optimize and finalize the meshing. Initially, uniform mesh was generated throughout the channel, which, based on flow regime of air bubbles, is optimised for the further study. Dense meshing was generated for both with and without injection of air till no change in final result is obtained. Optimized mesh is shown in Figure 27. For the simulation of three-dimensional, Implicit Unsteady Segregated flow, Volume of Fluid (VOF) approach was used to solve Reynolds Average Navier-Stokes Equations (RANS) and Eulerian multiphase equations of state with multiphase interactions based on density and surface tension of air and water. To account for the Boundary layer effect, Exact wall distance, Two layer all

y+ wall treatment and Realizable K-Epsilon Two Layer approach was effectively utilised. For the simulation of Turbulence, K- Epsilon Turbulence model was used. Velocity inlet boundary condition was used to setup the flow velocity of water at water inlet boundary. Similarly, for setting up of air inlet, mass flow rate boundary condition was used. At the outlet, pressure outlet boundary condition is used. For all other sides of channel, typical wall boundary condition with No Slip condition was used.

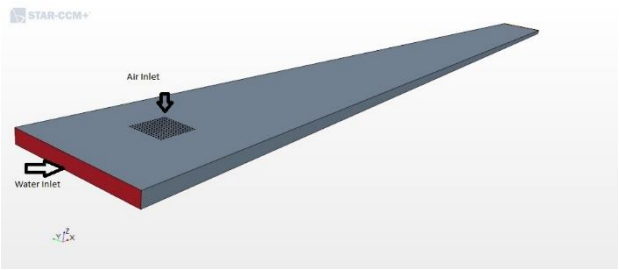

Figure 26 Geometry used for simulations

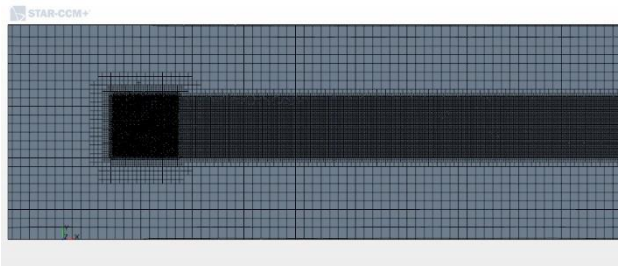

Figure 27 Optimised Mesh used for simulations

Figure 28 shows the comparison of C_{FO} values with experiment without injection of air at a location of 750mm from the injection point. Moreover, Figure 29 & Figure 30 shows the comparison of reduction in C_F values with experimental values, with and without injection of air at flow speed of 5m/s & 6m/s respectively. Here C_{FO} refers to coefficient of friction without the injection of bubbles and C_F refers to coefficient of friction with the injection of bubbles. Results obtained through CFD studies are in accordance with results obtained by experiments carried out by Moriguchi, et al, (2002), Kato, et al, (1998) and Madavan, et al, (1984).

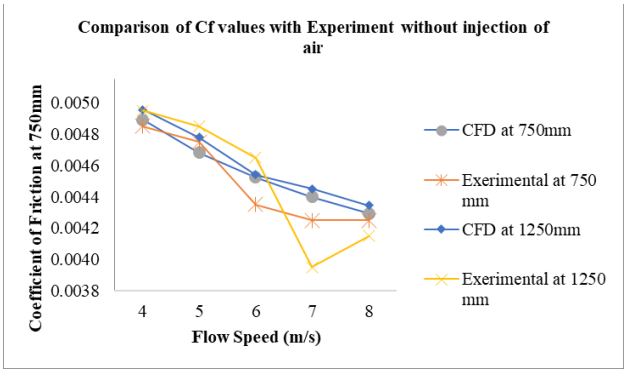

Figure 28 Comparison of CF values with experiment without injection of air

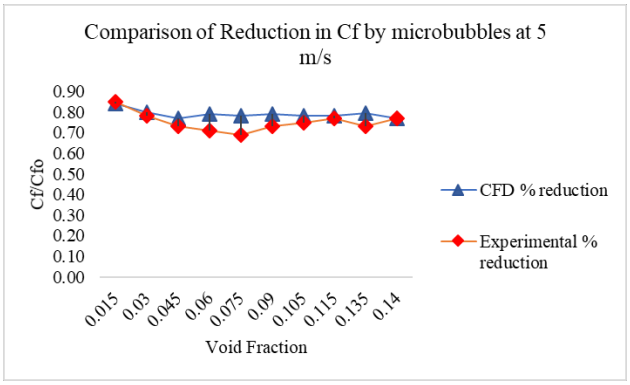

Figure 29 Comparison of reduction in CF with experiment, with and without injection of air at flow speed of 5m/s

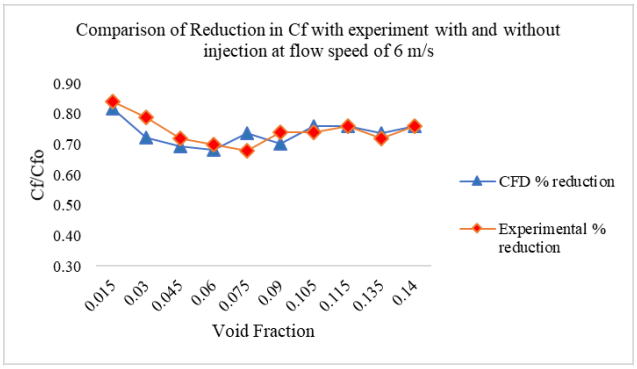

Figure 30 Comparison of reduction in CF with experiment, with and without injection of air at flow speed of 6m/s

12.2 VARIATION OF CF VALUES IN THE LONGITUDINAL DIRECTION FOR DIFFERENT SPEEDS & VF

Investigation on effect of flow speed on MBDR effect in longitudinal direction for different void fraction was carried out. From the Figure 31 & Figure 33, it can be concluded that, for Void fraction values of 3% and 9%, in general, MBDR effect is more for flow speed of 5m/s giving lowest values of coefficient of friction. However, as shown in Figure 32, MBDR effect was found to be maximum at higher speed of 7m/s at void friction of 6%. In most of the cases, MBDR effect reduced with increase in distance from the injection point, except for few cases at Void fraction of 9%, where in, MBDR effect increased from a point having distance 800mm onwards for speed of 7m/s and 600mm onwards for 4m/s. Reason for the same may be, as the distance increases in the longitudinal direction, bubbles coalesce with each other and form air pockets. This is the major reason for variation in C_F values in longitudinal direction, as bubbles coalesce to form air pockets avoiding any contact of water with the surface and thus reducing the coefficient of friction.

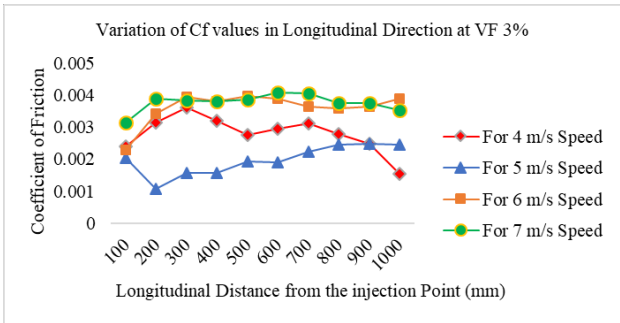

Figure 31 variation CF values in longitudinal direction for different flow speeds at VF of 3%

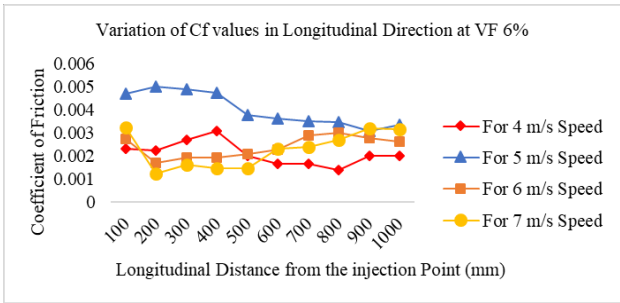

Figure 32 variation CF values in longitudinal direction for different flow speeds at VF of 6%

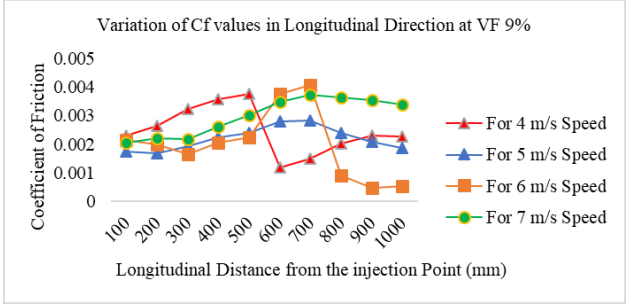

Figure 33 variation CF values in longitudinal direction for different flow speeds at VF of 9%

12.3 VARIATION OF C_F VALUES IN TRANSVERSE DIRECTION FOR DIFFERENT SPEEDS & VF

Similar investigation on effect of flow speed on MBDR effect in transverse direction for different values of void fraction was carried out. From the Figure 35 & Figure 36, it can be concluded that, for Void fraction values of 6% and 9%, MBDR effect is reduced with increase in distance from the injection point. For the case at Void fraction of 3% (Figure 34), similar observation was made for lower speeds of 4m/s and 5m/s, however, at higher speeds, due to more turbulence created, air bubbles distributed more in spanwise direction, causing increase in MBDR effect in spanwise direction.

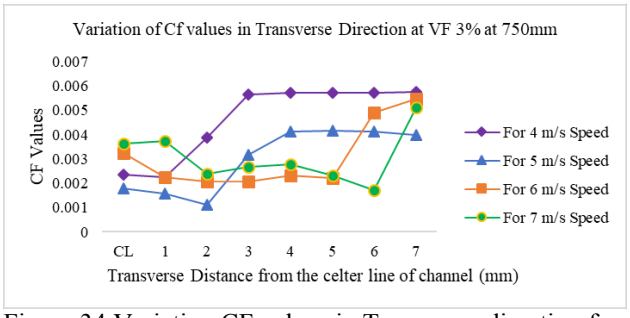

Figure 34 Variation CF values in Transverse direction for different flow speeds at VF of 3%

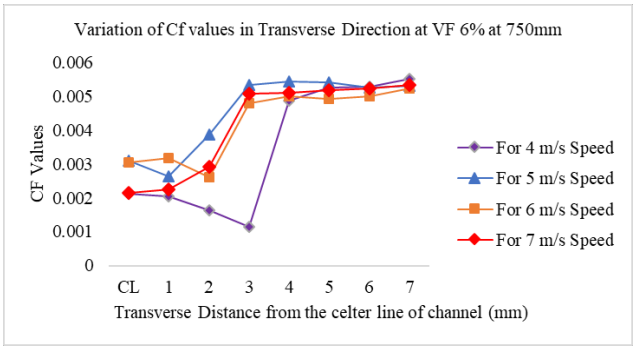

Figure 35 variation CF values in Transverse direction for different flow speeds at VF of 6%

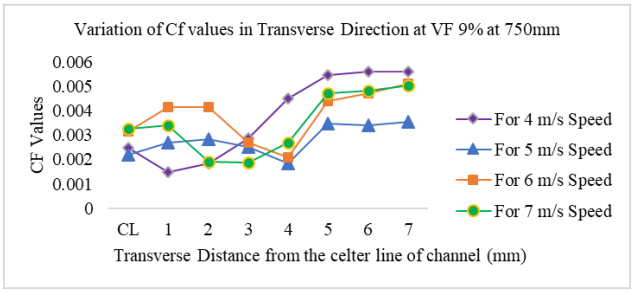

Figure 36 variation CF values in Transverse direction for different flow speeds at VF of 9%

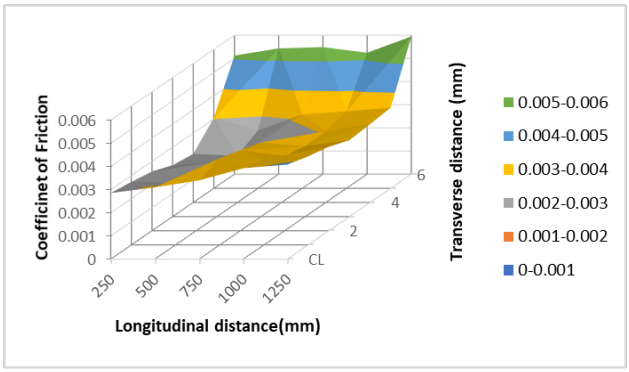

Figure 37 Variation of CF values at different longitudinal and transverse locations at flow speed of 6m/s and VF 11.5%

Figure 37 describes Variation of C_F values at different longitudinal and transverse locations at flow speed of 6m/s and VF of 11.5%, which clearly shows that, C_F value increases with increase in longitudinal and transverse distance from the air injection point. Moreover, it can be seen that, there is a variation in C_F values in longitudinal direction, which is mostly due to coalescence and breaking of bubbles with the distance from the injection point. To conclude, MBDR effect quickly reduces in the streamwise direction at immediate downstream of injection and gradually decreases further downstream. In the spanwise direction, there is no constant reduction region and the reduction effect reduces linearly towards the side end. Figure 38 describes the Longitudinal variation of C_F values for different values of void fraction. From the Figure 18, it can be concluded that, C_F value decreases till void fraction of 7.5%, beyond which, these values start increasing. This may be due the fact that, additional turbulence created by the injection of air bubbles. To conclude, as the MBDR effect depends upon the presence of Microbubbles, C_F values keep varying from point to point and do not follow a particular pattern.

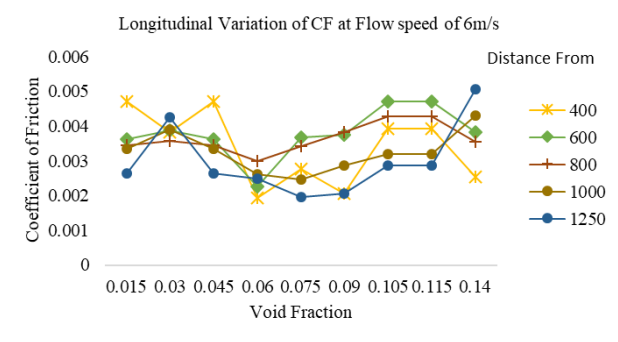

Figure 38 Longitudinal variation of CF at flow speed of 6m/s and different void fraction

To conclude, the distance from the injection point is the most important parameter in obtaining the reduction in frictional drag, and that the boundary layer thickness of top plate has little effect on the skin friction reduction by microbubbles. MBDR effect mostly depends on local void fraction than the injection void fraction. Local void fraction depends on the coalescence and breaking of bubbles. Formation of air pockets increases the local void fraction and in turn reduces coefficient of fraction, which has been found in many cases, where in, MBDR effect was found to be more after certain distance from the injection point

12.4 INVESTIGATION OF ALTERATION OF FLOW PARAMETERS AND C_F VALUES FOR DIFFERENT DEPTHS OF CHANNEL AT THE INJECTION POINT

It is well known fact that, diameters of microbubbles generated depends on the flow parameters at the injection point. Hence to investigate this effect, three different channels as used in experiments by (Morguchi & Kato, 2002) are modelled here in the CFD study. All three channels have the same test section height of 10 mm throughout the length except at the injection point. Channel 1, 2 & 3 have channel heights of 10mm, 5mm and 20mm at the injection point respectively. Channel 2 and Channel 3 are shown in Figure 39 along with velocity distribution throughout the length. Investigation has been carried out to check the changes in MBDR effect due to this variation in flow parameters for three different speeds of 5m/s, 6m/s and 7m/s at constant volume fraction of 6%.

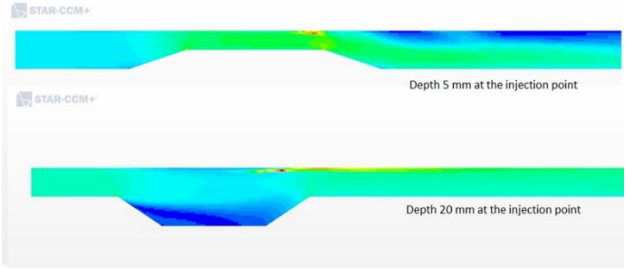

Figure 39 Channel 2 & 3 with velocity distribution

Figure 40 shows the variation of Void Fraction and in turn distribution of microbubbles for different depths of channel at the injection of point. As seen from the figure, for 5mm depth of the channel, due to reduction of pressure at the injection point, flow velocity increases which in turn causes increase in turbulence. This is forcing microbubbles to widely distribute in transverse direction and giving equal reduction in frictional drag in the transverse direction as well.

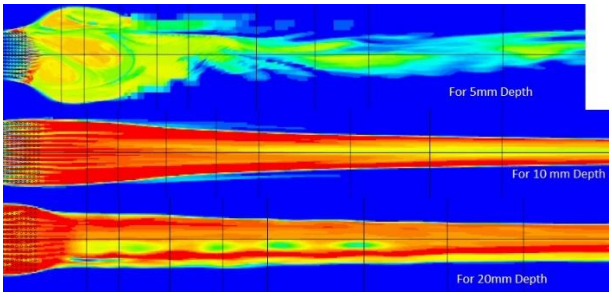

Figure 40 Variation of Void Fraction for different depths at the injection of point

Figure 41 depicts the variation of Turbulent Kinetic Energy for different depths at 750mm from the injection point. From the distribution, it is confirmed that, for 5mm depth of channel, as more number of bubbles are distributed in spanwise direction, turbulent kinetic energy reduces and for 20mm depth of channel, the same is increased due to injection of air. This implies that, out of three channels tested, channel with depth of 5mm gives best results to reduce frictional drag.

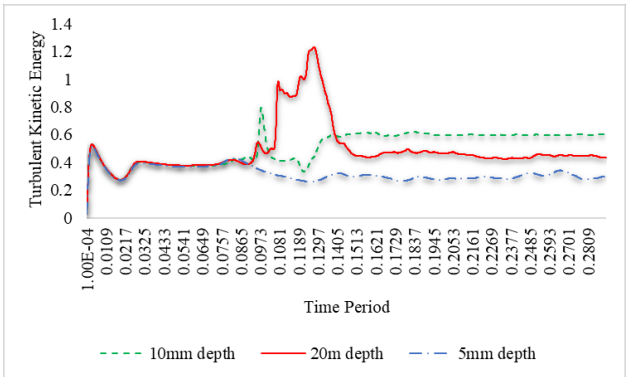

Figure 41 Variation of Turbulent Kinetic Energy for different depths at 750mm from the injection of point

Figure 42, Figure 43 & Figure 44 shows variation of C_F values in Transverse Direction at 750mm from the injection point and at constant value of Volume Fraction of 6% for different Flow Speeds of 5m/s, 6m/s and 7m/s respectively and of course for different depths of channel. From these figures, it can be safely concluded that, 5mm depth at the injection point gives best results for the MBDR effect, attaining minimum values of Coefficient of friction. Moreover, it can be seen that, for 5mm depth of channel, MBDR effect is almost equal in transverse direction. Also, it can be observed that, MBDR effect is maximum for lower flow speed of 5m/s as compared to other speeds. At higher flow speeds, additional turbulence created is increasing the turbulent viscosity and in turn the Reynolds stress.

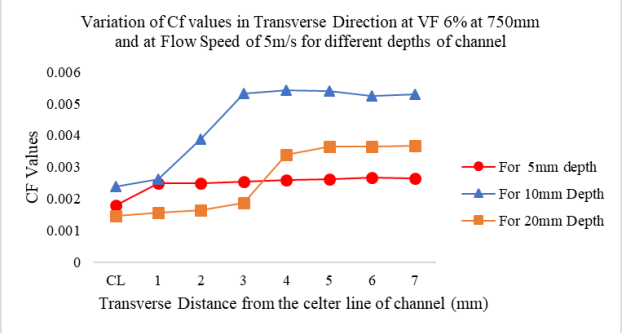

Figure 42: Variation of CF values in Transverse Direction at VF 6% at 750mm and at Flow Speed of 5m/s for different depths of channel

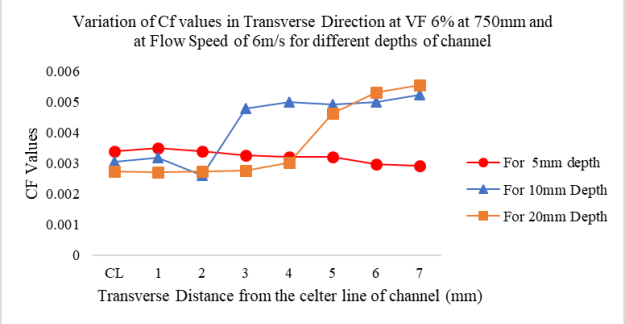

Figure 43: Variation of CF values in Transverse Direction at VF 6% at 750mm and at Flow Speed of 6m/s for different depths of channel

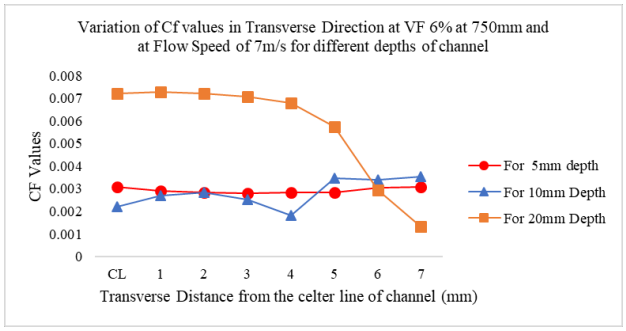

Figure 44 Variation of CF values in Transverse Direction at VF 6% at 750mm and at Flow Speed of 7m/s for different depths of channel

13. SUGGESTIONS TO IMPROVE THE DRAG REDUCTION/ FUTURE SCOPE FOR RESEARCHERS

Based on the exhaustive investigation carried out on MBDR studies carried out in past, following proposed concepts/opinions can become significant in increasing MDDR effect.

- As mentioned in the expression of net-work ratio (r_w), it is recommended to reduce ratio of wave drag to viscous drag (r_D), which implies that, one must choose a hull form that has small wave drag. The hull form of a large tanker is regarded suitable for MBDR method, as it has flat and very wide bottom, which will help the bubbles injected at the bow will stay close to the bottom due to the action of buoyancy.
- To increase MBDR effect, increase $F_d = \frac{U}{\sqrt{gD}}$, which can be implemented by reducing the depth at which the air bubbles needed to be injected.
- Moreover, reduce C_P, i.e., inject air at a location that has low pressure. This implies that, a ship operating in shallow water with micro bubbles injected will provide better results for MBDR method as compared to same ship operating in deep water.
- To re-develop or re-calibrate bubble coalescence based on the flow conditions.
- In the future, one can expect to carry out a detailed investigation into the bubble deformation effect to comprehensively clarify the mechanism of the frictional drag reduction due to microbubbles.
- Many researchers have struggled to investigate the effectiveness of micro bubbles on ships. Further research should be continued to enable the development of modification of turbulent boundary layer and thus increasing the ship efficiencies.
- Further studies of the hull features on the air-cavity boat performance, including aftbody deadrise, wetted skegs with finite width, multi-cavity setups, and propulsor is needed.
- Contradictory conclusions have been made based on the experimental results, which suggests that, there may be reduction in propulsive efficiency due to

microbubble injection. This needs further investigation.

- Experimentally validate the simulation results using towing tank experiments of ship model.
- One of the major problems faced in air lubricated methods is the uncontrolled bubble migration resulting in spending more energy for continuous bubble injection, which needs an urgent attention.
- Effect of SWR paint on the reduction can be further investigated, as, it is projected that, microbubbles will stick to the paint, however, it may also force liquid to stick to the paint and thus may increase the drag.
- Further study on comparison of reduction in drag by injecting bubbles at forward and/or midship of hull or at different locations may be carried out. Authors are of the opinion that, to increase effectiveness of MBDR, researchers can increase locations of injection points below the hull, which obviously needs further study.
- To study the effect of ALS in restricted area viz. motion in shallow water, restricted channel on reduction of frictional drag. Authors are of the opinion that, increase in drag for Inland and Coastal vessels where ship motion is restricted by channel width or depth will be compensated by reduction in friction frictional drag by MBDR. Moreover, motion in restricted area will assist the proper distribution of air bubbles below the hull.
- To Investigate the effect of microbubbles on the performance of propeller, cavitation and in turn the erosion, vibration, rudder control force reduction, echo sounder used by naval and research vessels.

14. CONCLUSIONS

The frictional resistance forms an integral part of total resistance of displacement ship of medium and low speed. Numerous technologies (Sindagi, et al, 2016), have been studied in past and utilized to reduce the frictional drag of a surface. It is concluded that, MBDR has added advantages over other drag reducing technologies, such as environmental friendly, easy operations, low costs and high saving of energy. It is also reported that, the MBDR is able to achieve 80% reduction in frictional drag, which can result in a substantial fuel savings for both commercial and naval ships. Literature review on MBDR suggests that, the skin friction reduction behaviour is a complicated phenomenon and depends on many factors such as Gas or Air Diffusion which depends on, Bubble size distributions and coalescence, which in turn depends on salinity of water, void fraction, location of injection points, depth of water in which bubbles are injected. To summarize, following inferences can be really vital in understanding the applying the methodology to reduce the frictional drag:

- Review opined that, MBDR effect is due to the alteration of local effective viscosity and density of the fluid which might reduce the Reynold's Stress. Bubble Stratification, near wall Phase composition, reduction of Turbulence intensity in the Streamwise direction, prevention of formation of spanwise vorticity near the wall are the other possible reasons.
- Diameter of bubbles depends mainly on flow parameters, which reduces by reducing the pressure at the point of injection. Pressure reduction can be achieved changing the height of channel or diameter of pipe at the injection point or by using venture tube.
- Detailed investigation on Bubble sizes and shapes after injection indicated that, bubble splitting is not dominant, however, bubble coalescence must be more prevalent as bubbles move downstream.
- MBDR effect quickly reduces in the streamwise direction at immediate downstream of injection and gradually decreases further downstream. In the spanwise direction, there is no constant reduction region and the reduction effect reduces linearly toward the side end. This suggests that, injected bubbles steadily diffuse toward side ends and are vanished steadily across them.
- The distance from the injection point is the most important parameter in obtaining the reduction in frictional drag and that the boundary layer thickness has little effect on the skin friction reduction by microbubbles
- It is found that the most important parameter in determining the fraction of drag reduction during gas injection is the effective void fraction, which is influenced by both, the injection rate and the static pressure under the test conditions.
- The formation of smaller bubbles, for the same gas injection rate, increased drag reduction when surfactant or salt exists in the aqueous environment.
- The reduction increases with increasing ship's length, as the benefit of the air injection extends to a greater fraction of the ship area downstream. Moreover, the cost of pumping the air goes as the square of the draft, since an increase in draft increases the back pressure against which the compressor or blower must work.

19. REFERENCES

1. ARNDT, R., HAMBLETON, W., KAWAKAMI, E. & AMROMIN, E. L., 2009. *Creation and Maintenance of Cavities Under Horizontal Surfaces in Steady and Gust Flows*. Journal of Fluids Engineering, Volume 131.
2. BUTUZOV, A., 1967. *Artificial cavitation flow behind a slender wedge on the lower surface of a horizontal wall*.. Fluid Dynamics, Volume 3, pp. 56-58.
3. BUTUZOV, A., SVERCHKOV, A., POUSTOSHNY, A. & CHALOV, S., 1999. *State of art in investigations and development for the ship on the air cavities*. China, International Workshop on Ship Hydrodynamics.

4. CECCIO, S. L., 2010. *Friction Drag Reduction of External Flows with Bubble and Gas Injection*. Annual Review of Fluid Mechanics, Volume 42, pp. 183-203..
5. ELBING, B. R. et al., 2008. *Bubble-induced skin-friction drag reduction and the abrupt transition to air-layer drag reduction*. Journal of Fluid Mechanics, Volume 612, pp. 201-236.
6. FOETH, E., n.d. *Decreasing frictional resistance by air lubrication*. Netherlands, 20th International Hiswa Symposium on Yacht Design and Yacht Construction & Maritime Research Institute of the.
7. FUKUDA, K. et al., 2000. *Frictional drag reduction with air lubricant over a super-water repellent surface*. J Mar Sci Technol, Volume 5, p. 123–130.
8. GOKCAY, S., INSEL, M. & ODABASI, A. Y., 2004. *Revisiting artificial air cavity concept for high speed craft*. Ocean Engineering, Volume 31, pp. 253-267.
9. JINHO, J. et al., 2014. *Experimental investigation of frictional resistance reduction with air layer on the hull bottom of a ship*. Int. J. Nav. Archit. Ocean Eng, Volume 6, pp. 363-379.
10. KANAI, A. & MIYATA, H., 2001. *Direct numerical simulation of wall turbulent flows with microbubbles*. Int. J. Numer. Meth. Fluids, Volume 35, pp. 593-615.
11. KATO, H. & KODAMA, Y., 2003. *Microbubbles as a Skin Friction Reduction Device - A Midterm Review of the Research, Japan:* Center for Smart Control of Turbulence National Maritime Research Institute, Japan.
12. KATO, H., MIURA, K., *YAMAGUCHI, H. & MIYANAGA, M., 1998. Experimental study on microbubble ejection method for frictional drag reduction*. J Mar Sci Technol, Volume 3, pp. 122-129.
13. KAWABUCHI, M. et al., 2011. CFD *Predictions of Bubbly Flow around an Energy-saving Ship with Mitsubishi Air Lubrication System*. Mitsubishi Heavy Industries Technical Review, 48(1).
14. KAWASHIMA, H. et al., n.d. *Experimental study of frictional drag reduction by microbubbles: Laser measurement and bubble generator,* Tokyo, Japan: Center for Smart Control of Turbulence, National Maritime Research Institute.
15. KIM, J., 2011. *Physics and control of wall turbulence for drag reduction*. Phil. Trans. R. Soc. A, pp. 1396-1411.
16. KITAGAWA, A. et al., n.d. *Turbulence structures of microbubble flow measured by PIV/PTV and LIF techniques*. Japan, Smart Control of Turbulence, Ministry of Education, Culture, Sports, Science and Technology.
17. KITAGAWA, A., HISHIDA, K. & KODAMA, Y., 2005. *Flow structure of microbubble-laden turbulent channel flow measured by PIV combined with the shadow image technique*. Experiments in Fluids, Volume 38, pp. 466-475.
18. KODAMA, Y. et al., 2004. *Practical application of microbubbles to ships - Large scale model experiments and a new full scale experiment*. National Maritime Research Institute, Toyo University, Azuma Shipping, Osaka Univ & Chugoku Marine Paints.
19. LAY, K. A. et al., 2010. *Partial cavity drag reduction at high Reynolds numbers*. Journal of Ship Research, 54(2), pp. 109-119.
20. LEWIS, E. V., n.d. *Principles of Naval Architecture, Second Revision*. Volume II Resistance & Propulsion. s.l.:Library of Congress Catalog Card No. 88-60829 ISBN No. 0-939773-01-5.
21. MADAVAN, K., DEUTSCH, S. & MERKLE, C. L., 1983. *Reduction of Turbulent Skin Friction by Microbubbles*. Technical Memorandum, The Pennsylvania State University, 9 MARCH, pp. File No. TM 83-23.
22. MADAVAN, K., DEUTSCH, S. & MERKLE, C. L., 1985. *Numerical Investigations Into the Mechanisms of Microbubble Drag Reduction*. Transactions of the ASME, Volume 107, pp. 370-377.
23. MADAVAN, K., DEUTSCH, S. & MERKLE, C. L., 24 Aug 1984. *Measurements of local skin friction in a microbubble modified turbulent boundary layer,* s.l.: echnical Memorandum, File No. TM 84-136, The Pennsylvania State University.
24. MÄKIHARJU, S. A., PERLIN, M. & CECCIO, S. L., 2012. *On the Energy Economics of Air Lubrication Drag Reduction*. Inter J Nav Archit Oc Engng, 4(4), pp. 412-422.
25. MÄKIHARJU, S. et al., 2010. *Perturbed Partial Cavity Drag Reduction at High Reynolds Numbers*. Pasadena, CA, Proc. 28th Symp. on Naval Hydrodynamics,.
26. MARIN, 2011. *The efficacy of air-bubble lubrication for decreasing friction resistance*. MARITECH NEWS, pp. 118-122.
27. MATVEEV, K. I., 2003. *On the limiting parameters of artificial cavitation*. Ocean Engineering, Volume 30, pp. 1179-1190.
28. MCCORMICK, M. & BHATTACHARYYA, R., 1973. *Drag reduction of a submersible hull by electrolysis*. Naval Engineering Journal 85, pp. 11-16.
29. MIZOKAMI, S. et al., 2010. *Experimental study of air lubrication method and verification of effects on actual hull by means of sea trial*. Mitsubishi Heavy Ind Techn Rev, 47(3), p. 41–47.
30. MOHANARANGAM, K., CHEUNG, S. C. P., TU, J. Y. & CHEN, L., 2009. *Numerical simulation of microbubble drag reduction using*

population balance model. Ocean Engineering, Volume 36, pp. 863-872.

31. MORIGUCHI, Y. & KATO, H., 2002. *Influence of microbubble diameter and distribution on frictional resistance reduction*. J Mar Sci Technol, Volume 7, pp. 79-85.
32. SANDERS, W. C. et al., 2006. *Bubble friction drag reduction in a high-Reynolds-number flat-plate turbulent boundary layer*. J. Fluid Mech, Volume 552, pp. 353-380.
33. SHEN, X., CECCIO, S. L. & PERLIN, M., 2006. *Influence of bubble size on micro-bubble drag reduction*. Experiments in Fluids, Volume 41, pp. 415-424.
34. SHEN, X., CECCIO, S. & PERLIN, M., 2006. *Influence of bubble size on microbubble drag reduction*. Exp Fluids, Volume 41, p. 415–424.
35. SINDAGI, S., VIJAYKUMAR, R. & SAXENA, B. k., 2016. *Frictional Drag Reduction: An EFD and CFD Based Review of Mechanisms*. IIT Madras, India, International conference on EFD and CFD – MARHY 2016.
36. SUNARYO, Y. G. & JAMALUDDIN, A., 2012. *Micro-bubble Drag Reduction on a High Speed Vessel Model*. J. Marine Sci. Appl, Volume 11, pp. 301-304.
37. TAKAHASHI, T. et al., 2001. *Mechanisms and Scale Effects of Skin Friction Reduction by Microbubbles*, Japan: Ship Research Institute, Shipbuilding Research Association of Japan.
38. THOMAS, I., KRISHNAN, R. G., SALOOP, T. S. & VISHNU M, M., 2016. *Mechanisms and Factors Affecting Microbubble Drag Reduction in Ship*. IOSR Journal of Mechanical and Civil Engineering (IOSR-JMCE), 13(3), pp. 97-102.
39. WATANABE M, 1991. *Air pollution from ship engines in maritime Transport*. Mar Eng Soc Jpn 26 (9).
40. WINKEL, E. S., CECCIO, S. L., DOWLING, D. R. & PERLIN, M., 2004. *Bubble-size distributions produced by wall injection of air into flowing freshwater, saltwater and surfactant solutions*. Experiments in Fluids, Volume 37, p. 802–810.
41. WU, S.-J., OUYANG, K. & SHIAH, S.-W., 2008. *Robust design of microbubble drag reduction in a channel flow using the Taguchi method*. Ocean Engineering, Volume 35, p. 856–863.
42. YOSHIAKI, K., AKIRA , K., TAKAHITO , T. & HIDEKI, K., 2000. *Experimental study on microbubbles and their applicability to ships for skin friction reduction*. International Journal of Heat and Fluid Flow 21, pp. 582-588.
43. YOSHIAKI, K. et al., n.d. *Drag Reduction of Ships by Microbubbles*. National Maritime Research Institute of Japan.
44. ZVERKHOVSKYI, O. et al., 2015. s.l.: MARIN Academy, Wageningen, NL; MARIN, Wageningen, NL Delft University of Technology, NL ; DAMEN Shipyards Gorinchem, NL.